Electronic Research Archive

ERA, 31(6): 3435–3452.
DOI: 10.3934/era.2023174
Received: 07 March 2023
Revised: 11 April 2023
Accepted: 12 April 2023
Published: 19 April 2023

http://www.aimspress.com/journal/ERA

Research article

Optimized LSTM based on improved whale algorithm for surface subsidence deformation prediction

Ju Wang[1], Leifeng Zhang[2,*], Sanqiang Yang[2], Shaoning Lian[1], Peng Wang[1], Lei Yu[1] and Zhenyu Yang[2]

[1] Beijing Municipal Road and Bridge Co., LTD., Beijing, China
[2] Hebei Civil Engineering Monitoring and Evaluation Technology Innovation Center, College of Civil Engineering, Hebei University, Baoding, Hebei, China

* **Correspondence:** Email: 635077193@qq.com.

Abstract: In order to effectively control and predict the settlement deformation of the surrounding ground surface caused by deep foundation excavation, the deep foundation pit project of Baoding City Automobile Technology Industrial Park is explored as an example. The initial population approach of the whale algorithm (WOA) is optimized using Cubic mapping, while the weights of the shrinkage envelope mechanism are adjusted to avoid the algorithm falling into local minima, the improved whale algorithm (IWOA) is proposed. Meanwhile, 10 benchmark test functions are selected to simulate the performance of IWOA, and the advantages of IWOA in learning efficiency and convergence speed are verified. The IWOA-LSTM deep foundation excavation deformation prediction model is established by optimizing the input weights and hidden layer thresholds in the deep long short-term memory (LSTM) neural network using the improved whale algorithm. The IWOA-LSTM prediction model is compared with LSTM, WOA-optimized LSTM (WOA-LSTM) and traditional machine learning, the results show that the final prediction score of the IWOA-LSTM prediction model is higher than the score of other models, and the prediction accuracy is better than that of traditional machine learning.

Keywords: deep foundation pit; deep learning; whale optimization algorithm; numerical simulation; short and long term memory; settlement prediction

1. Introduction

Presently, above-ground resources can no longer meet people's needs, and urban construction has gradually shifted to underground development [1]. As a result, the size and depth of foundation pits have grown in recent years [2], the risk of foundation pit excavation construction also rises gradually [3]. Therefore, it is the main task at present to control and predict the settlement deformation during the excavation of deep foundation pits to provide reference for construction, so as to effectively ensure construction safety [4].

With the rapid rise of intelligent algorithms [5], many data processing methods have achieved better applications in foundation pit deformation prediction [6]. Among them, the representative ones are neural network model, gray model, support vector machine model (SVM), etc. Meng Guo [7] et al. used BP neural network rolling prediction method for the horizontal displacement of the enclosure structure, which is more suitable for practical engineering. Zhang Zhenghu [8] et al. combined the gray model with the time series analysis method to extract the trend terms of slope displacements using the improved GM(1,1) to transform the non-smooth time series into smooth time series for ARMA or AR time series analysis. Zhou Y [9] et al. substituted the data and risk levels of different monitoring items into the random forest model to obtain the relationship between foundation pit monitoring values and safety risks. Su W [10] et al. proposed the method of SVM model to determine the risk level to assess the risk during the construction of foundation pits. These data mining methods have achieved some results, but they also have limitations. For example, BP neural network is an optimization method for local search, but the problem it wants to solve is to solve the global extrema of complex functions, and the algorithm has the problem of falling into local extremums, making training failure; support vector machine model has better prediction effect, but it is prone to the problem of difficult parameter selection.

Based on this, Hinton [11] proposed a deep learning approach. Compared to traditional machine learning, it has strong learning ability, feature extraction does not rely on manual, can map arbitrary functions, and can solve very complex problems. RNN (recurrent neural network) is a kind of deep learning, which can effectively deal with sequence data, but there is a serious short-term memory problem. LSTM is improved based on RNN, which can effectively retain for long-term information and solve the long sequence training. There are problems with vanishing gradients and gradient explosions during this process. Hong Yuchao [12] et al. used a combined CNN-LSTM neural network to predict the ground surface, and proved that this neural network with integrated consideration of spatio-temporal characteristics is more accurate than a single LSTM neural network in predicting results. Zhang Zhenkun [13] et al. exploited the multi-head attention mechanism combined with LSTM to make dynamic prediction of landslide, the results showed that the prediction accuracy was greatly improved.

WOA [14] mimics the social behavior of whales. The algorithm employs a bubble net search strategy. It has the advantages of less parameter setting, better search ability and simple mechanism compared with traditional methods. Although using WOA to tune the input weights and hidden layer thresholds of LSTM can make the model accuracy improve [15], however, there is still a problem that the algorithm is prone to fall into the local minimum value and the convergence speed is slow [16].

In view of the above problems, this paper proposes a new method to optimize LSTM based on IWOA. This method uses Cubic mapping to optimize the initial selection method of whale algorithm to improve the optimization-seeking efficiency, while adjusting the weights of the shrinkage envelope

mechanism to avoid the algorithm falling into local minima points, optimizes input weights and hidden layer thresholds in the depth-length short-term memory neural network using the IWOA to establish the IWOA-LSTM deep foundation excavation deformation prediction model.

2. Background

The study was based on the pipe jacking work well for the drainage project of Yong Hua Street (South Second Ring Road - Tai Hang Road) of the Great Wall Automobile Technology Industrial Park municipal road construction project located in Baoding City. The excavation depth of the pit reached 10.38 m, and the perimeter of the pit was about 80 m. The slope was made of 80-thick C20 shotcrete surface layer with 16 mm diameter reinforcement, and the length of the reinforcement was 1.2 m. As shown in Figure 1. The site of the foundation pit is shown in Figure 2.

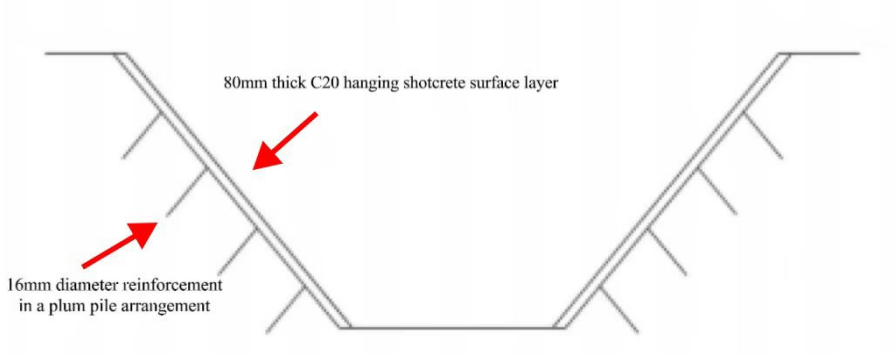

Figure 1. Foundation pit support section.

Figure 2. Site plan of foundation pit.

The soil parameters obtained according to the geological survey report provided by the construction unit are shown in Table 1.

Table 1. Parameters of soil layer.

Soil layer	Thickness/ m	Volumetric weight/ （kN·m-	Cohesion /kPa	Angle of internal friction/	Natural moisture content/%	Natural porosity ratio/%	Liquid moisture limit/%	Plastic limit water content/%
Vegetative fill	0.30～1.00	18.8	17.5	22.9	19.6	0.641	27.3	17.7
Powdered earth	2.40～7.40	19.3	18.4	21.9	18.2	0.691	27.1	17.5
Powdery clay	0.80～1.90	19.4	16.1	21.9	19.6	0.718	27.5	17.9
Powdered earth	1.00～2.50	19.6	19.4	21.7	18.6	0.691	27.4	17.4
Fine Sand	2.00～7.80	19.5	17.2	21.1	17.5	0.705	27.2	17.5

The project monitored the settlement of the surrounding buildings, the surrounding surface settlement, the deep horizontal displacement and the slope earth pressure from the beginning to the completion of the construction, and the monitoring point arrangement is shown in Figure 3. The surface settlement curve is shown in Figure 4.

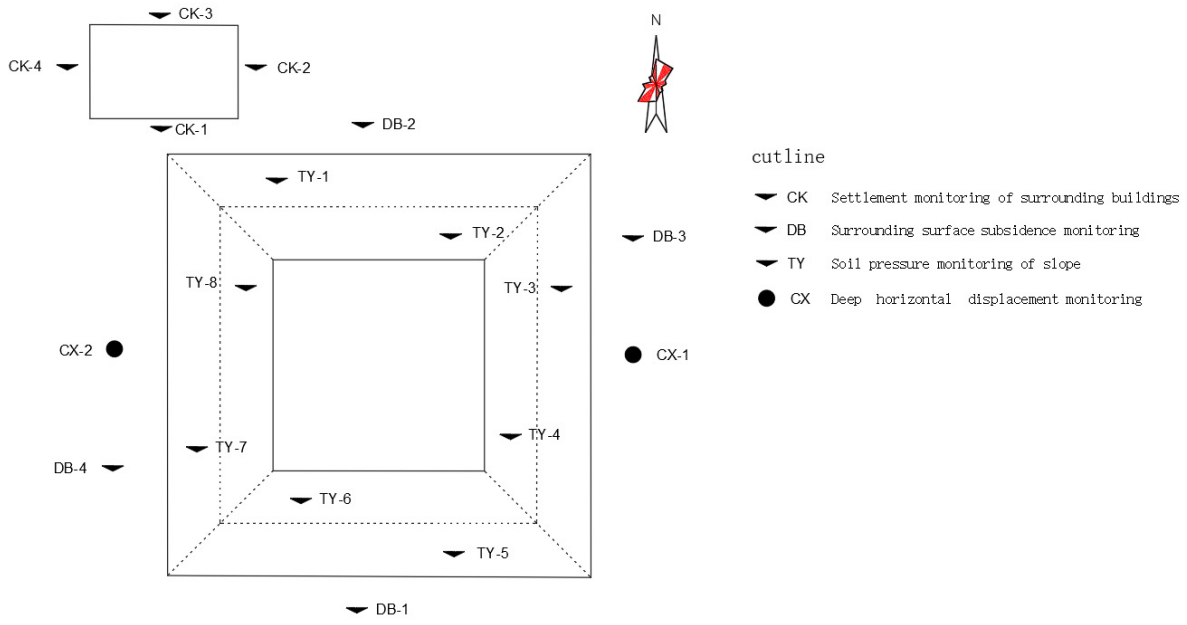

Figure 3. Monitoring point plan layout.

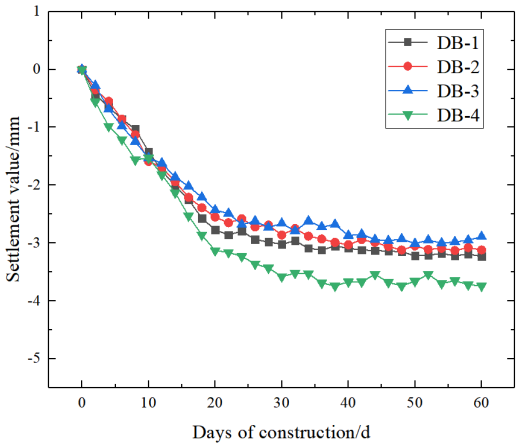

Figure 4. Surface settlement curve.

As can be seen from Figure 4, the settlement of DB-1, DB-2, DB-3 and DB-4 monitoring points generally increases with the increase of excavation depth. In addition, the settlement rate is relatively high at the initial stage of excavation, and the settlement is basically stable until the excavation reaches the bottom of the pit and a period of time thereafter. In this monitoring, the maximum settlement value of the surface monitoring point is DB-4, reaching about 3.74 mm, and the minimum settlement value is DB-3. The reason is that the DB-4 point is close to the construction foundation pit, which is greatly affected. At the same time, it can be seen that the surface settlement curve has an obvious inflection point after the foundation pit anchor is applied on the 18th day of construction, indicating that the surface settlement is affected by the foundation pit support.

3. Research methods

3.1. Deep long and short term memory neural network

The LSTM was proposed by Hochrieter [17], it was proposed and also improved, and the network basic unit is shown in Figure 5 [18].

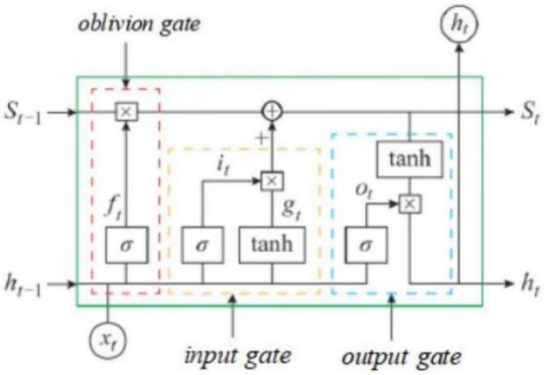

Figure 5. LSTM neural network basic unit.

After continuous improvement, the current LSTM calculation method is as follows:

$$o_t = \sigma\left(W_{ox}x_t + W_{oh}h_{t-1} + b_o\right) \tag{1}$$

$$f_t = \sigma\left(W_{fx}x_t + W_{fh}h_{t-1} + b_f\right) \tag{2}$$

$$g_t = \phi\left(W_{gx}x_t + W_{gh}h_{t-1} + b_g\right) \tag{3}$$

$$i_t = \sigma\left(W_{ix}x_t + W_{ih}h_{t-1} + b_i\right) \tag{4}$$

$$S_t = g_t \odot i_t + S_{t-1} \odot f_t \tag{5}$$

$$h_t = \phi\left(S_t\right) \odot o_t \tag{6}$$

where, f_t, i_t, g_t, o_t, h_t and S_t are respectively the states of forgetting gate, input gate, input node, output gate, intermediate output and state unit; $W_{fx}, W_{fh}, W_{ix}, W_{ih}, W_{gx}, W_{gh}, W_{ox}$ and W_{oh} are the matrix weights of the corresponding gate multiplied by the input and intermediate output, respectively; b_f, b_i, b_g, b_o are the corresponding weight coefficient matrix. $\odot$ means multiplying the elements of a vector by bits; σ indicates the change of sigmoid function; ϕ is the change in the tanh function.

3.2. The whale optimization algorithm

Whales are considered to be the largest mammals on Earth and can think, choose and cooperate [14]. However, what is most remarkable is their hunting technique. Humpback whales create special bubbles along the spiraling circle to complete their hunting, and eventually surround the fish on the surface of the ocean in an optimal way to catch prey [19]. WOA is an intelligent optimization algorithm that simulates this special hunting method. This predation can be described as three periods: surround the prey, bubble net predation and hunt for prey [20].

1) Surround the prey

The position of the candidate solution in this stage, $\vec{X}(t+1)$, is determined by the following formula:

$$\vec{D} = \left|\vec{C}.\vec{X}^* - \vec{X}(t)\right| \tag{7}$$

$$\vec{X}(t+1) = \left|\vec{X}^*(t) - \vec{A}.\vec{D}\right| \tag{8}$$

where, $\vec{X}(t)$ is the current position, $\vec{X}^*(t)$ is the best candidate solution in the current iteration, and t is the number of iterations. $\vec{A}$ and $\vec{C}$ is determined by the following formula:

$$\vec{A} = \left|2\vec{a}.\vec{r} - \vec{a}\right| \tag{9}$$

$$\vec{C} = 2.\vec{r} \tag{10}$$

where, $\vec{r}$ is a random vector in $[0,1]$, and $\vec{a}$ is a parameter decreasing from 2 to 0 as the number of iterations increases, defined as

$$a = 2 - 2t / T \tag{11}$$

T is the maximum number of iterations

2) Hunt for prey

In the stage of searching prey, when A meets $|A| \geq 1$, whales update their positions according to each other's positions. so that the algorithm acquires a certain amount of global optimality-seeking capability. The location is determined by the following equation:

$$\vec{D} = \left|\vec{C}.\vec{X}_{rand} - \vec{X}(t)\right| \tag{12}$$

$$\vec{X}(t+1) = \left|\vec{X}_{rand}(t) - \vec{A}.\vec{D}\right| \tag{13}$$

where, $\vec{X}_{rand}(t)$ represents the position vector of randomly selected whales in the population.

3) Bubble net predation

During a bubble net attack, humpbacks use two strategies simultaneously: narrowing the circle and spiraling, which shrinks the circle as the spiral travels. In the whale algorithm, the shrink surround mechanism is realized by reducing the a value in Eq (11). The spiral travel formula is as follows:

$$\vec{X}(t+1) = \vec{D}'.e^{bl}.\cos(2\pi l) + \vec{X}^*(t) \tag{14}$$

where $\vec{D}' = \left|\vec{X}^*(t) - \vec{X}(t)\right|$ represents the distance between the whale and its prey, which is the distance between the ith candidate solution and the best solution in the current iteration. b is the constant that defines the helix equation, $l \in [-1,1]$.

Whales shrink the encircling and swim along the spiral path toward the prey. In order to synchronize these two behaviors, WOA assumes that the probability of choosing spiral rotation and shrinking the encircling is 0.5 during the hunting process at this time, and the bubblenet predation model is expressed as

$$\vec{X}(t+1) = \begin{cases} \vec{X}^*(t) - \vec{A} \cdot \vec{D}, p < 0.5 \\ \vec{D}'.e^{bl}.\cos(2\pi l) + \vec{X}^*(t), p \geq 0.5 \end{cases} \tag{15}$$

3.3. Improved whale optimization algorithm

Because the traditional WOA has the problems of easily falling into local minima, low efficiency of optimization and the problems of slow convergence speed, so using Cubic mapping mode of initial population of WOA algorithm is optimized to ensure the diversity of initial population, adjust the adaptive weight at the same time, avoid algorithm trapped in local minimum points, improve the whale algorithm (IWOA) [21]. Its expression is:

$$x_{n+1} = \rho x_n \left(1 - x_n^2\right) \tag{16}$$

where $x_n \in (0,1)$, ρ are mapping factors.

For the adaptive weights are adjusted as shown in the following equation.

$$w = w_{\min} + (w_{\max} - w_{\min}) \cdot mm \cdot e^{-\frac{t}{\max gen}} \tag{17}$$

where mm is the adjustment factor and $\max gen$ is the number of iterations.

Cubic mapping initial selection method, compared with the original selection method, IWOA has a more uniform initial position distribution, which ensures the diversity of the initial population and improves the defect that the algorithm is easy to fall into local extremes, thus improving the efficiency of the algorithm for finding the best [22].

3.4. IWOA-LSTM prediction model flow

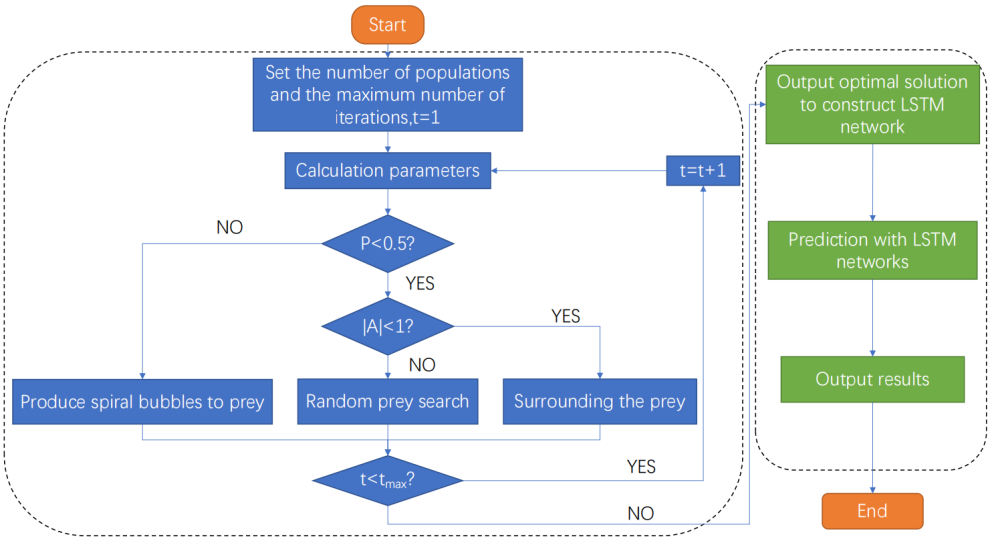

Figure 6. Flow chart of IWOA-LSTM model.

WOA mainly relies on the coefficient vector $\vec{A}$ to select the path to search for prey and uses the probability p to decide the final predation mechanism [23], and the computational flow of IWOA-LSTM is shown in Figure as follows.

Step 1: Set the initial parameters

Step 2: Calculate $p, |A|$. Determine if p is less than 50%, if yes, go to the next step, otherwise use Eq (14) for position update.

Step 3: judge if $|A|$ is less than 1, yes then use Eq (8) for position update; otherwise use Eq (13) for the position update.

Step 4: Determine whether it is the optimal solution.

Step 5: Determine whether t_{max} has been achieved if not, go back to step 2.

Step 6: Output the optimal solution and construct the LSTM network with the output parameters.

Step 7: Perform prediction with the constructed LSTM network [24].

4. IWOA-LSTM predictive model application

4.1. IWOA performance analysis

Table 2. Benchmark function expressions.

Function expressions	Dimensionality	Search interval	$f_{\min}$
$f_1(x)=\sum_{i=1}^{D}x_i^2$	30	[-100,100]	0
$f_2(x)=\sum_{i=1}^{D}\lvert x_i\rvert \div \prod_{i=1}^{D}\lvert x_i\rvert$	30	[-100,100]	0
$f_3(x)=\sum_{i=1}^{D}\left(\sum_{j=1}^{i}x_j\right)^2$	30	[-100,100]	0
$f_4(x)=\max_i\left(\lvert x_i\rvert\right),1\le i\le D$	30	[-50,50]	0
$f_5(x)=\sum_{i=1}^{D-1}\left[100\left(x_{i+1}-x_i^2\right)^2+\left(x_i-1\right)^2\right]$	30	[-30,30]	0
$f_6(x)=\sum_{i=1}^{D}ix_i^4+random[0,1]$	100	[-10,10]	0
$f_7(x)=\sum_{i=1}^{D}\left(\lvert x_i+0.5\rvert\right)^2$	100	[-100,100]	0
$f_8(x)=\sum_{i=1}^{D}-x_i\sin\left(\sqrt{\lvert x_i\rvert}\right)+418.9829\times D$	100	[-500,500]	0
$f_9(x)=\sum_{i=1}^{D}\left[x_i^2-10\cos\left(2\pi x_i\right)\div 10\right]$	100	[-10,10]	0
$f_{10}(x)=-20\exp\left(-0.2\sqrt{\frac{1}{D}\sum_{i=1}^{D}x_i^2}\right)$	100	[-50,50]	0

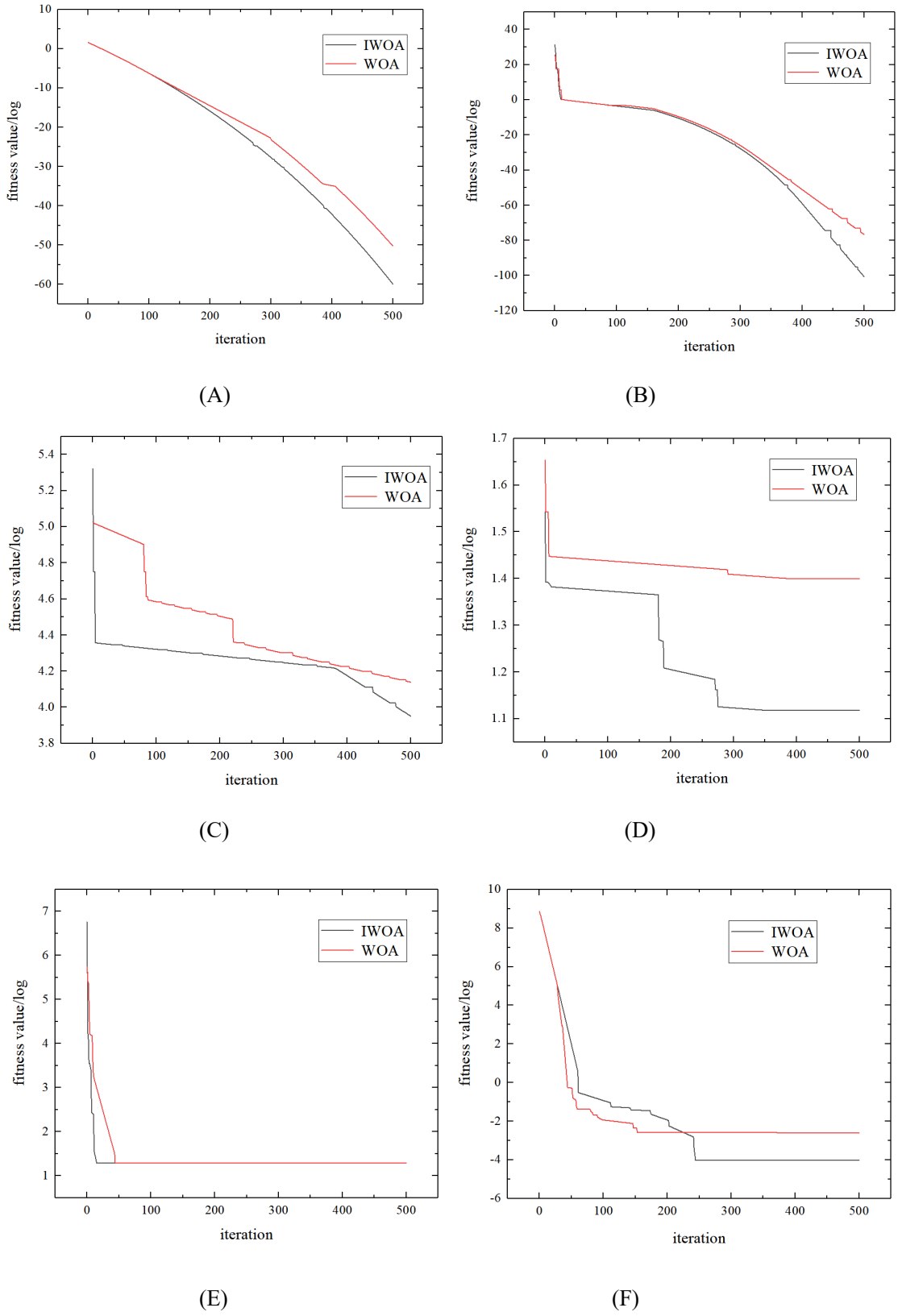

continued on next page

Figure 7. Convergence curve of each test function.

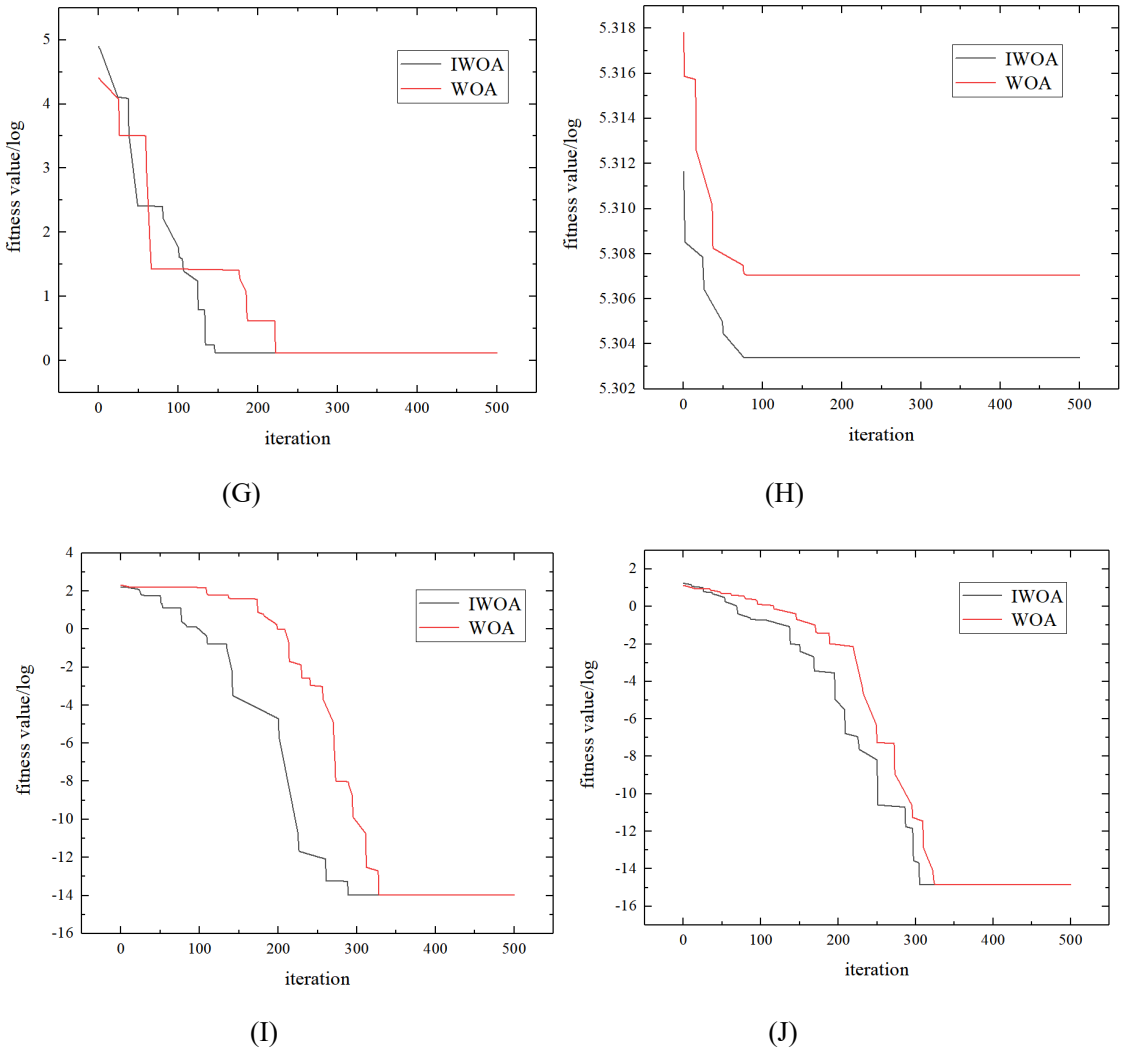

Figure 7. Convergence curve of each test function.

To assess the performance of the IWOA, the improved whale algorithm performance is tested by simulation with the 10 benchmark functions shown in Table 2. The benchmark functions are shown in Table 2 [25]. The maximum number of iterations is set to 500 times, the number of populations is set to 30, and the optimized values of the test function are all 0. The optimal iterative convergence curve is shown in Figure 7 [26].

The abscissa in Figure 7 is the number of iterations. The smaller the vertical coordinate, the higher the convergence accuracy of the algorithm [27]. As can be known from the Figure 7, IWOA algorithm during the entire process of search has faster convergence speed and higher convergence precision. This proves that the Cubic mapping is used to optimize the initial population selection method of the IWOA algorithm, which makes the distribution of the initial position of the improved population more uniform and increases the diversity of the population position [28]. These improvements make weights in the IWOA alter automatically according to current conditions [29]. As a result, IWOA obtains a faster optimization speed than WOA during the initial iteration, and can balance the utilization ability of other positions while optimizing [30].

In this study, the optimized hyperparameters of LSTM model were set as follows:"Hidden layers = 2", "Number of neurons in the first layer = 115", "Number of second layer neurons = 55", "Dropout = 0.2", "epoch = 11", and "batch-size = 256".

4.2. Model evaluation

In this paper, three evaluation tools are used to evaluate and analyze the final prediction results, namely, MAE, RMSE and ARER [31].

$$MAE = \frac{1}{n}\sum_{i=1}^{n}\left|\hat{S}(x) - f(x)\right| \tag{18}$$

$$RMSE = \sqrt{\frac{\sum_{i=1}^{n}\left[\hat{S}(x) - f(x)\right]^2}{n}} \tag{19}$$

$$ARER = \frac{1}{n}\sum_{i=1}^{n}\left|\frac{\hat{S}(x) - f(x)}{f(x)}\right| \times 100\% \tag{20}$$

where $\hat{S}(x)$ is the predicted value, $f(x)$ is the true value, and n is the number of samples.

4.3. Predicted results

In order to demonstrate the superiority of IWOA-LSTM prediction model, the IWOA-LSTM, BPNN, CNN, LSTM, GRU, WOA LSTM six kinds of prediction model is used in the comparison test [32]. The settlement value of a settlement monitoring point at a certain time is used as a sample, and there are 180 samples at each monitoring point, 720 samples in total. The 720 samples were randomly sorted, and 504 samples of the top 70% were selected as the training set, and 216 samples of the remaining 30% were selected as the test set [33]. The comparison of predicted results are shown in Figure 8. The comparison curve of prediction errors of different models are shown in Figure 9. Figure 10 shows the final score of model prediction accuracy.

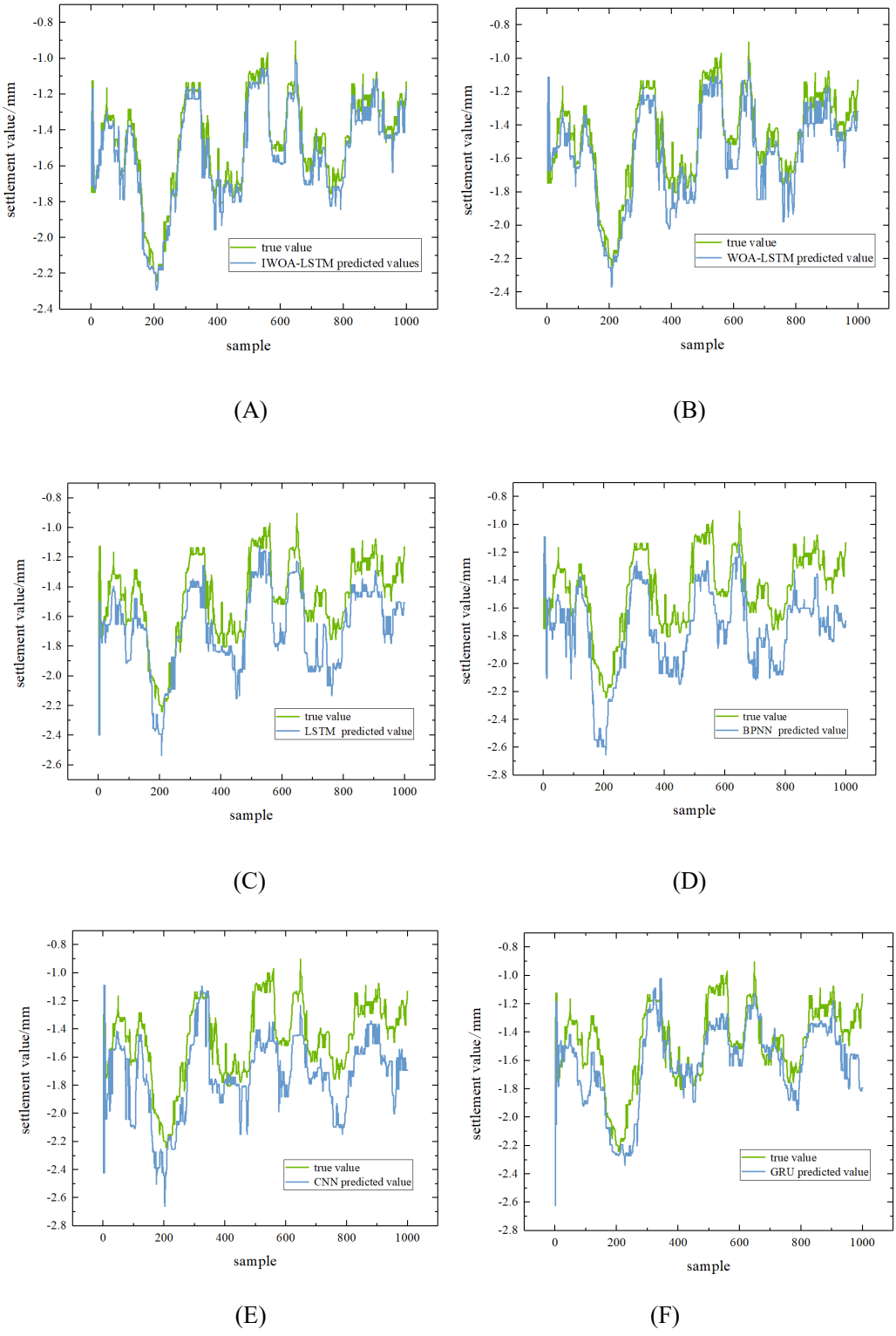

Figure 8. Comparison of predicted results.

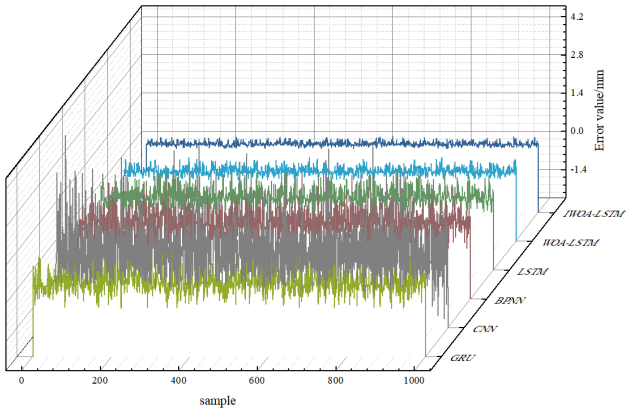

Figure 9. Prediction error curves of different models.

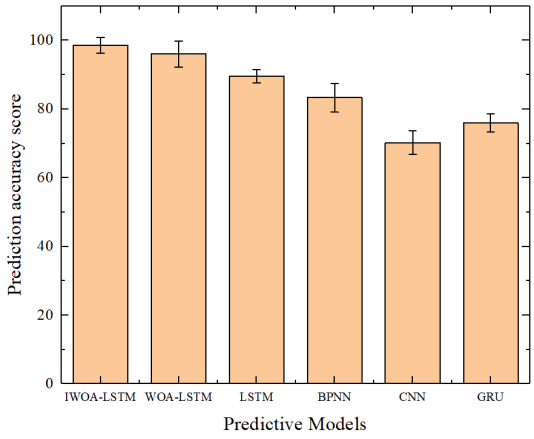

Figure 10. Prediction accuracy scores of different models.

Table 3. Precision comparison of models.

Predictive Models	MAE	RMSE	ARER
IWOA-LSTM	0.13451	0.25689	3.1403
WOA-LSTM	0.23456	0.31457	4.0195
LSTM	0.61257	0.78892	8.9024
BPNN	0.69874	0.83724	9.3514
CNN	0.83753	0.9536	12.3371
GRU	0.62648	0.79345	10.0237

As can be known from the above figure, the IWOA-LSTM has higher accuracy than the traditional machine learning, WOA-LSTM and LSTM prediction models. Table 3 shows the comparison of MAE, RMSE, and ARER of the predicted model.

MAE, RMSE and AERE of the IWOA-LSTM prediction model are 0.13451, 0.25689 and 3.1403, respectively, which are better than WOA-LSTM, LSTM, BPNN, CNN and GRU. This shows that the IWOA-LSTM has a better prediction effect compared to the other forecasting methodology.

5. Conclusions

In this paper, we use Cubic mapping to optimize the initial population selection method, while the weights of the shrinkage envelope mechanism are adjusted, and the input weights and hidden layer thresholds in the deep long and short term memory neural network are optimized using the improved whale algorithm to establish an IWOA-LSTM deep foundation excavation deformation prediction model. It is also validated with the deep foundation pit project of Baoding Automobile Technology Industrial Park, and compared with traditional machine learning. The following conclusions are drawn.

1) IWOA can effectively optimize the initial population selection method, thus ensuring the diversity of the initial population, while adjusting the weights of the shrinkage bracketing mechanism, which can avoid the algorithm from falling into local minimal value points.

2) The convergence performance of IWOA is tested with 10 test functions. IWOA has higher convergence accuracy than WOA. Compared with WOA-LSTM model, IWOA-LSTM model takes less computing time and has faster convergence rate.

3) The final prediction score of the IWOA-LSTM prediction model proposed in this paper is 98.8721, MAE, RMSE and ARER index were 0.13451, 0.25689 and 3.1403, respectively, which is better than the other five prediction models mentioned in this paper, indicating that the IWOA-LSTM has higher prediction accuracy.

Foundation pit accident is a serious safety accident in building construction. It can cause huge economic losses and put workers' lives at risk. Therefore, it is necessary to predict the surface settlement of foundation pit. The results of this study show that it is feasible to use IWOA-LSTM model to analyze and predict.

These predictions can effectively reflect the development trend of future foundation pit surface settlement and provide scientific basis for construction units to take safety measures in advance. Due to the limitation of the data in this study, the influence of load around the foundation pit and mechanical excavation vibration was not considered. In future studies, more comprehensive data attributes will be collected to improve the predictive accuracy of the model.

Acknowledgments

This research was supported by the Natural Science Foun-dation of Hebei Province (E2018201106), Hebei Provincial Department of Transportation science and technology project (PHP-C34200-2503631-1), and the Beijing Municipal Road and Bridge Scientific Research Project (ERDC0026).

Conflict of interest

The authors declare there is no conflict of interest.

References

1. C. Feng, D. Zhang, Sandy pebble in subway station foundation pit overall deformation model and its application, *Chin. J. Rock Mech. Eng*., **S2** (2018), 4395–4405. http//:doi.org/10.13722/j.carolcarroll nki jrme. 2018.0722.
2. X. Cao, X. Lu, Y. Gu, Study on axial pressure variation of steel support in deep foundation pit, *Chin. J. Geotech. Eng.*, **44** (2022), 1988–1997. http//:doi.org/10.11779/CJGE202211004
3. K. Cheng, R. Xu, H. Ying, B. Li, X. Gan, Z. Qiu, et al., Experimental study on excavation characteristics of a large 30.2m deep foundation pit in Hangzhou soft clay area, *Chin. J. Rock Mech. Eng*., **40** (2021), 851–863. http//:doi.org/10.13722/j.cnki.jrme.2020.0636
4. G. Zheng, Deformation control method and engineering application of foundation pit in soft soil area, *Chin. J. Geotech. Eng.*, **44** (2022), 1–36+201. http//:doi.org/10.11779/CJCE202201001
5. X. Ni, C. Wang, D. Tang, Early warning and inducement analysis of super-large deformation of deep foundation pit in soft soil area, *J. Cent. South Univ. (Sci. Technol.)*, **53** (2022), 2245–2254. http//:doi.org/10.11817/j.issn.1672-7207.2022.06.025
6. S. Qiao, Z. Cai, Z. Zhang, Characteristics of soft soil Long and narrow deep foundation pit retaining system in Nansha Port Area, *J. Zhejiang Univ., Eng. Sci.*, **56** (2022), 1473–1484. http//:doi.org/10.3785/j.issn.1008-973X.2022.08.001
7. G. Meng, J. Liu, J. Huang, Research on horizontal displacement prediction of deep foundation pit envelope based on BP artificial neural network, *Urban Rapid Rail Transition*, **35** (2022), 80–88. http//:doi.org/10.3969/j.issn.1672-6073.2022.03.013
8. Z. Zhang, M. Yuan, J. Deng, S. Xue, Slope displacement prediction based on improved grey-timeseries analysis time-varying model, *Chin. J. Rock Mech. Eng*., **33** (2014), 3791–3797. http//:doi.org/10.13722/j.cnki.jrme.2014.s2.049
9. Y. Zhou, S. Li, C. Zhou, Intelligent approach based on random forest for safety risk prediction of deep foundation pit in subway stations, *J. Comput. Civil Eng.*, **33** (2019), 05018004. https://doi.org/10.1061/（ASCE）CP.1943-5487.0000796
10. Y. Zhou, W. Su, L. Ding, Predicting safety risks in deep foundation pits in subway infrastructure projects: support vector machine approach. *J. Comput. Civil Eng.*, **31** (2017), 04017052. https://doi.org/10.1061/（ASCE）CP.1943-5487.0000700
11. G. Hinton, R. Salakhutdinov, Reducing the dimensionality of data with neural networks, *Science*, **313** (2006), 504–507. https://doi.org/10.1126/science.1127647
12. Y. Hong, J. Qian, Y. Ye, Application of CNN-LSTM Model based on Spatial-temporal correlation characteristics in deformation prediction of foundation pit engineering, *Chin. J. Geotech. Eng.*, **43** (2021), 108–111. https://doi.org/10.11779/CJGE2021S2026
13. Z. Zhang, D. Zhang, J. Li, Research on LSTM-MH-SA landslide displacement prediction model based on multi-head self-attention mechanism, *Rock Soil Mech.*, **43** (2022), 477–486+507. https://doi.org/10.16285 / sm j.r.2021.2091
14. S. Mirjalili, A. Lewis, The whale optimization algorithm, *Adv. Eng. Software.*, **95** (2016), 51–67. https://doi.org/10.1016/j.advengsoft.2016.01.008

15. J. Nasiri, F. M. Khiyabani, A whale optimization algorithm (WOA) approach for clustering, *Cogent Math. Stat.*, **5** (2018), 1483565. https://doi.org/10.1080/25742558.2018.1483565
16. S. Chakraborty, S. Sharma, A. K. Saha, S. Chakraborty, SHADE–WOA: A metaheuristic algorithm for global optimization, *Appl. Soft Comput.*, **113** (2021), 107866. https://doi.org/10.1016/j.asoc.2021.107866
17. S. Hochreiter, J. Schmidhuber, Long short-term memory, *Neural Comput.*, **9** (1997), 1735–1780. https://doi.org/10.1162/neco.1997.9.8.1735
18. S. Yang, D. Chen, S. Li, Carbon price forecasting based on modified ensemble empirical mode decomposition and long short-term memory optimized by improved whale optimization algorithm, *Sci. Total. Environ.*, **716** (2020), 137117. https://doi.org/10.1016/j.scitotenv.2020.137117
19. Z. Zhao, W. Chen, X. Wu, LSTM network: a deep learning approach for short-term traffic forecast, *IET Intell. Transp. Syst.*, **11** (2017), 68–75. https://doi.org/10.1049/iet-its.2016.0208
20. S. Mostafa, S. Yazdani, IWOA: An improved whale optimization algorithm for optimization problems, *J. Comput. Des. Eng.*, **6** (2019), 243–259. https://doi.org/10.1016/j.jcde.2019.02.002
21. N. Xu, X. Wang, X. Meng, Gas concentration prediction based on IWOA-LSTM-CEEMDAN residual correction model, *Sensors*, **22** (2022), 4412. https://doi.org/10.3390/s22124412
22. Z. Zhuang, X. Zheng, Z. Chen, T. Jin, A reliable short-term power load forecasting method based on VMD-IWOA-LSTM algorithm, *IEEJ Trans. Electr. Electron. Eng.*, 2022. https://doi.org/10.1002/tee.23603
23. X. Liu, Y. Bai, C. Yu, Multi-strategy improved sparrow search algorithm and application, *Math. Comput.*, **96** (2022). https://doi.org/10.3390/mca27060096
24. A. Chhabra, S. Sahana, N. Sani, A. Mohammadzadeh, H. Omar, Energy-Aware Bag-of-Tasks scheduling in the cloud computing system using hybrid oppositional differential evolution-enabled whale optimization algorithm, *Energies*, **15** (2022), 4571. https://doi.org/10.3390/en15134571
25. Y. Qi, Z. Cheng, Research on traffic congestion forecast based on deep learning, *Information*, **14** (2023), 108. https://doi.org/10.3390/info14020108
26. W. Guo, Y. Mao, Y. Chen, X. Zhang, Multi-objective optimization model of micro-grid access to 5G base station under the background of China's carbon peak shaving and carbon neutrality targets, *Energy Res.*, **10** (2022), 1032993. https://doi.org/10.3389/fenrg.2022.1032993
27. W. Lu, H. Rui, C. Liang, L. Jiang, S. Zhao, K. Li, A method based on GA-CNN-LSTM for daily tourist flow prediction at scenic spots, *Entropy*, **22** (2022), 261. https://doi.org/10.3390/e22030261
28. D. Li, Z. Li, K. Sun, Development of a novel soft sensor with long short-term memory network and normalized mutual information feature selection, *Math. Probl. Eng.*, (2020), 1–11. https://doi.org/10.1155/2020/761701
29. W. Sun, J. Wang, X. Wei, An improved whale optimization algorithm based on different searching paths and perceptual disturbance, *Symmetry*, **10** (2018), 210. https://doi.org/10.3390/sym1006021
30. Y. Li, W. Pei, Q. Zhang, Improved whale optimization algorithm based on hybrid strategy and its application in location selection for electric vehicle charging stations, *Energies*, **15** (2022), 7035. https://doi.org/10.3390/en15197035
31. X. Cui, S. E, D. Niu, D. Wang, M. Li, An improved forecasting method and application of China's energy consumption under the carbon peak target, *Sustainability*, **13** (2021), 8670. https://doi.org/10.3390/su13158670

32. B. Khan, P. Singh, Selecting a meta-heuristic technique for smart micro-grid optimization problem: A comprehensive analysis, *IEEE Access*, **5** (2017), 13951–13977. https://doi.org/10.1109/ACCESS.2017.2728683
33. Y. Zhang, R. Li, J. Zhang, Optimization scheme of wind energy prediction based on artificial intelligence, *Environ. Sci. Pollut. Res.*, **28** (2021), 39966–39981. https://doi.org/10.1007/s11356-021-13516-2

AIMS Press